Vol. 55: 17–32, 2012
doi: 10.3354/cr01127

CLIMATE RESEARCH
Clim Res

Published November 15

Diurnal, seasonal, and altitudinal trends in microclimate across a tropical montane cloud forest

Joshua M. Rapp[1,3,*], Miles R. Silman[1,2]

[1]Department of Biology and [2]Center for Energy, Environment, and Sustainability, Wake Forest University, Winston-Salem, North Carolina 27106, USA

[3]*Present address:* Harvard Forest, Harvard University, Petersham, Massachusetts 01366, USA

ABSTRACT: Altitudinal gradients are often used as natural laboratories to study ecosystem dynamics, biodiversity, and species' distribution response to climate gradients. However, the underlying climate gradients are rarely described in detail, especially in the tropics. In this study, we describe the diurnal and seasonal patterns in microclimate across a 3900 m altitudinal gradient in and adjacent to the Kosñipata Valley in Manu National Park, Peru, on the eastern slope of the tropical Andes. We focus on the understudied altitudinal range between 1500 and 3500 m using micrometeorological data associated with a permanent tree plot network designed to study cloud forest biodiversity and ecosystem dynamics. Data from this plot network were supplemented with data in the public domain across a 20 000 km^2 area with time series at individual sites lasting from 2 to 17 yr. Observed diurnal and seasonal trends in microclimate variables were explained by diurnal and seasonal variation in solar radiation and atmospheric moisture flux. Altitudinal trends in microclimate varied seasonally, with solar radiation, vapor pressure deficit, and temperature reaching their annual maximum earlier at higher altitudes, likely because of seasonally shifting cloud dynamics. Cloud dynamics were important in determining diurnal, seasonal, and altitudinal trends in several microclimate variables, suggesting that changes to cloud frequency and altitudinal occurrence associated with global climate change could have important impacts on cloud forest ecosystem dynamics, in addition to those of rising temperatures.

KEY WORDS: Tropical montane cloud forest · Andes · Altitudinal gradient · Seasonality · Climate change · Cloud dynamics

1. INTRODUCTION

Altitudinal gradients as climate gradients have played a central role in the history of ecology and biogeography (Lomolino 2001), but the underlying climate gradients have rarely been described in detail. A detailed understanding of how climate changes across altitudinal gradients is needed, especially in the humid tropics, where tropical montane cloud forest, an understudied ecosystem, is common. Unique features of cloud forests, compared to adjacent lowland forests, include decreased forest stature, thick (often described as xeromorphic) leaves, low tree growth rates and forest productivity, thick humic or peat soils, and heavy accumulations of epiphytes in the forest canopy (Leigh 1975, Grubb 1977, Vitousek 1998, Foster 2001). These features are linked to persistent cloud cover and the microclimate variables influenced by clouds, including light, rain, temperature, and humidity. Understanding how these variables change across altitudinal gradients is a first step towards understanding how microclimate affects montane forest ecology and hydrology. Data describing cloud forest climates are sparse, and where they exist are usually for isolated locations (e.g. Grubb & Whitmore 1966, Fleischbein et al. 2006, Gomez-Peralta et al. 2008, Giambelluca et al. 2009, Holwerda et al. 2010). Published data on tropical altitudinal gradients

*Email: rapp.joshua@gmail.com

are few and mostly from oceanic islands such as Hawaii (Kitayama & Mueller-Dombois 1994) and Borneo (Aiba & Kitayama 2002), although a recent study along an altitudinal gradient in Bolivia (Gerold et al. 2008) provided data for a continental site. There is an urgent need for these data, as cloud forests are especially vulnerable to climate change (Still et al. 1999, Foster 2001, Herzog et al. 2011).

Future climate scenarios predict drying trends in much of the tropics (Neelin et al. 2006), and climate model projections for the Andes predict warmer temperatures and lower precipitation in the dry season (Vuille et al. 2008, Martinez et al. 2011). Of particular concern is the possibility of a rising cloud base, which has been linked to the extinction of cloud forest animal species in Costa Rica (Pounds et al. 1999), and is predicted to adversely affect epiphytes (Nadkarni & Solano 2002). The lifting condensation level, which influences the height at which clouds form, is predicted to rise by 1000 m or more over the Amazon by 2100 (Cowling et al. 2008, Pinto et al. 2009). The location of the cloud base defines the lower limit of cloud forest (Leigh 1975, Grubb 1977, Foster 2001), and is associated with changes in forest structure, such as the sharp changes in biomass and productivity of trees (Girardin et al. 2010) and epiphytic bryophytes (A. Howrath unpublished data) between 1500 and 2000 m, seen at our study area in the Andes.

The upper limit of cloud forest is generally determined by the altitudinal tree line. Tree line is an obvious ecotone on mountains worldwide, with climatic, edaphic, and anthropogenic factors implicated in determining tree line location (Korner 1998, Smith et al. 2009). In the tropical Andes, anthropogenic fire has been implicated in enforcing current tree line (Sarmiento & Frolich 2002, Bader & Ruijten 2008). One outstanding question is why these high altitudes support fire when the cloud forest below is almost continuously saturated. The 'trade wind inversion', a layer of warm, dry air above the moist layer of surface air, has been implicated in defining the upper limit of cloud forest in Hawaii (Kitayama & Mueller-Dombois 1994, Loope & Giambelluca 1998). An inversion has also been identified at our study area, the altitude of which varies seasonally, reaching a minimum in the dry season (Halladay 2012).

While most cloud forests are found in coastal climates and continental mountains tend to be drier (Jarvis & Mulligan 2011), the vast swath of cloud forest along the eastern margin of the tropical Andes of South America (Bubb et al. 2004, Bruijnzeel et al. 2011) provides a notable exception. Northeast trade winds bring moisture from the tropical Atlantic across the Amazon Basin, but are blocked from continuing westward by the Andes. The barrier is enhanced by dry, cold air over the high Andes, set in place by persistent subsidence over coastal western South America, which promotes the development of the Bolivian high over the Altiplano in summer (Garreaud et al. 2009). Blocked from continuing westward, the warm air mass turns south along the Andean front to form the South American Low-level Jet (SALLJ; Marengo et al. 2004). Local topography and the dry air mass to the west interact with the SALLJ to produce dry and wet spots in the eastern Andes (Killeen et al. 2007), supporting a diversity of forest types. Incursions of cold, dry air moving north along the Andes from southern South America can happen throughout the year. These events, locally termed 'friajes,' can lead to temperature drops of up to 10°C in the subtropics east of the Andes (Garreaud 2000). Cooling is greatest during austral winter incursions, and below the 700 hPa level, although temperature anomalies are found through most of the troposphere (Garreaud 2000). These incursions are likely to have ecological effects (e.g. Doan 2004), but little is known about them.

Here we describe daily, seasonal, and altitudinal trends in microclimate of a 3900 m continental altitudinal gradient, extending from the western Amazonian lowlands to above tree line in the eastern Andes. We focus on the cloud forest portion of the altitudinal gradient (1500–3500 m), while including data from meteorological stations in the adjacent lowland and highland areas. We describe the climate across the putative cloud base and near the tree line, to examine whether there are strong changes in microclimate at these locations that would explain the observed changes in forest structure. We also examine the upslope propagation of several cold air incursion events. Continuous data for a 1 yr period are described in detail for the core part of the gradient, and are compared to supplementary data with time series of up to 17 yr. While the short time series of our data limit our ability to generalize about the climate of the study area, the altitudinal trends in microclimate at daily and seasonal scales are instructive in the context of regional climate.

2. MATERIALS AND METHODS

2.1. Study site

Since 2003, the Andes Biodiversity and Ecosystem Research Group (ABERG) has established a network

of 1 ha permanent tree plots and accompanying micrometeorological sensors in the Kosñipata Valley (13° 6′18″ S, 71° 35′ 21″ W), in and adjacent to Manu National Park in southeastern Peru. Additional data were obtained from weather stations maintained by the Peruvian government or biological field stations in the Kosñipata Valley and adjacent areas in the Andean highlands and western Amazonian lowlands (Fig. 1, Table 1). The Kosñipata Valley is within the Tambopata-Manu wet spot, as described by Killeen et al. (2007). Vegetation in the region ranges from moist tropical rainforest in the lowlands to tropical montane cloud forest at mid-elevations, to puna (high-elevation grassland) above the tree line. Cloud forests on the east Andean slopes are part of a biodiversity hotspot (Gentry 1988, 2006, Myers et al. 2000.

2.2. Sensors

Daily maximum and minimum temperature and precipitation totals were available from 4 micrometeorological stations in the Kosñipata Valley maintained by the Servicio Nacional de Meteorolgía e Hidrología del Perú (Table 1) and micrometeorological stations at 3 lowland sites, 1 cloud forest site, and 1 highland site from the Atrium Biodiversity Information System. In addition, ABERG installed HOBO micrometeorological sensors (Onset Computer) from June 2007 to September 2009 along 2 ridges that form the northern boundary of the Kosñipata Valley. Here we focus on data from July 2007 to June 2008, the period for which data were most continuous. HOBO Pro V2 Temperature/Relative Humidity Data Loggers (U23-001; factory calibration accuracy: ±0.2°C/±2.5–3.5%), were installed on tree trunks approximately 1 m above the soil surface in the forest understory at locations that would minimize exposure to direct sunlight which could result in higher temperature and lower relative humidity readings. Data were logged every 10 or 15 min. HOBO Microstation Data Loggers (H21-002) outfitted with Temperature/Relative Humidity Smart Sensors (S-THB-M002; factory calibration accuracy: ±0.2°C/±2.5–3.5%) with radiation shields, 0.2 mm Rainfall Smart Sensors (S-RGB-M002; factory calibration accuracy: ±1.0%), Photosynthetic Light Smart Sensors (S-LIA-M003; factory calibration accuracy: ±5 µmol m^{-2} s^{-1}/± 5.0%), and Wind Speed and Direction Smart Sensors (S-WCA-M003; factory calibration accuracy: ±0.5 m^2 s^{-1}/±5°) were mounted on poles approximately 1 m above the forest canopy, and data were logged every 10 min.

2.3. Analysis

2.3.1. Temperature

For data from automatic micrometeorological sensors, we first calculated minimum, maximum, mean, mean daytime (06:00–18:00 h), and mean nighttime (18:00–06:00 h) temperatures for each day using all

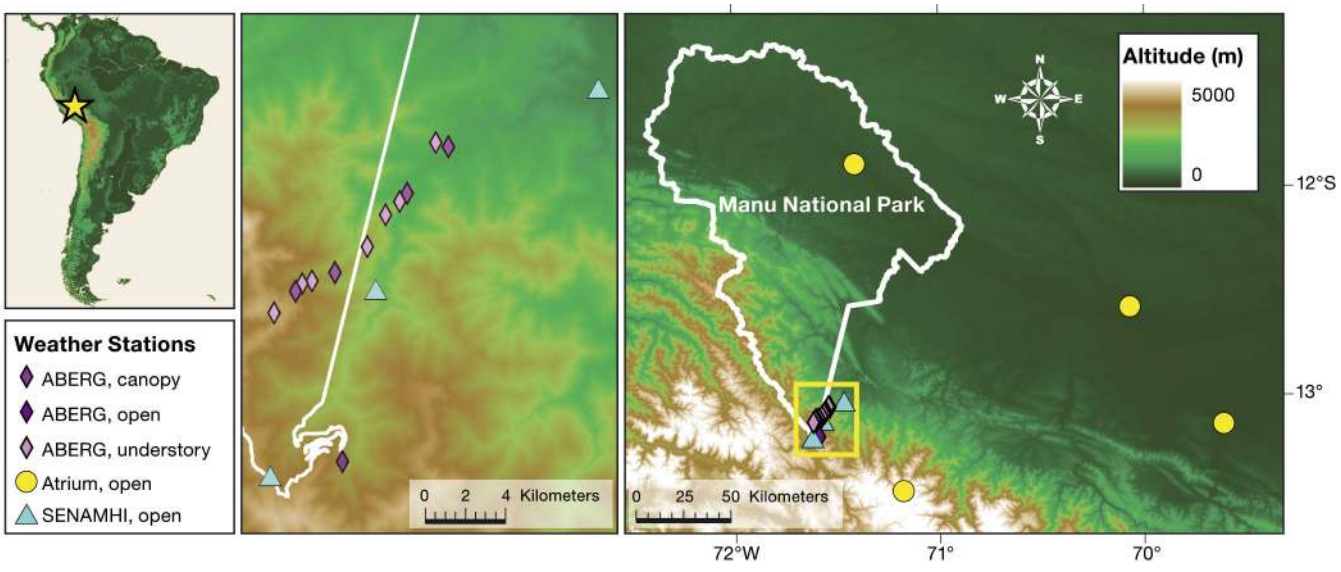

Fig. 1. Weather stations and sensors in the Kosñipata Valley, Peru, and adjacent areas. Andes Biodiversity and Ecosystem Research Group (ABERG) stations and sensors that are not labeled were installed in or near permanent tree plots. Location names are listed in Table 1

Table 1. Weather stations and sensors in the Kosñipata Valley and adjacent areas, showing data source (Andes Biodiversity and Ecosystem Research Group, ABERG, plot network; Atrium Biodiversity Information System of the Botanical Research Institute of Texas data portal, Atrium: atrium.andesamazon.org; or data from the Servicio Nacional de Meteorolgía e Hidrología del Perú, SENAMHI: www.senamhi.gob.pe), and years of data collection (data are not continuous for all years for most sensors). WS: weather station, RH: relative humidity

Site	Altitude	Location	Sensor	Source	Latitude (°W)	Longitude (°S)	Years
Tambopata	230	Open	Manual WS	Atrium	13.137	69.612	1995–2008
Los Amigos	280	Open	Manual WS	Atrium	12.5768	70.0691	2000–2009
Cocha Cashu	340	Open	Manual WS	Atrium	11.8884	71.4072	1984–2001
Chontachaca	982	Open	Manual WS	SENAMHI	13.02389	71.46778	2000–2008
SP_1500	1500	Canopy	Automatic WS	ABERG	13.04928	71.53672	2007–2009
SP_1500	1500	Understory	Temp/RH	ABERG	13.04928	71.53672	2007–2009
SP_1750	1750	Understory	Temp/RH	ABERG	13.04733	71.54245	2007–2009
TU_1800	1840	Canopy	Automatic WS	ABERG	13.06990	71.55582	2007–2009
TU_1800	1840	Understory	Temp/RH	ABERG	13.06990	71.55582	2007–2009
Rocotal	2010	Open	Manual WS	SENAMHI	13.11333	71.57083	2000–2008
TU_2000	2020	Understory	Temp/RH	ABERG	13.07373	71.55935	2007–2009
TU_2250	2250	Understory	Temp/RH	ABERG	13.07958	71.56592	2007–2009
TU_2500	2520	Understory	Temp/RH	ABERG	13.09380	71.57445	2007–2009
TU_2750	2720	Canopy	Automatic WS	ABERG	13.10517	71.58937	2007–2009
TU_2750	2720	Understory	Temp/RH	ABERG	13.10550	71.58928	2007–2009
WA_3000	3000	Open	Automatic WS	ABERG	13.1903	71.5869	2006–2009
TU_3000	3020	Understory	Temp/RH	ABERG	13.10905	71.59998	2007–2009
TU_3250	3200	Understory	Temp/RH	ABERG	13.11023	71.60442	2007–2009
TU_3450	3400	Canopy	Automatic WS	ABERG	13.11347	71.60757	2007–2009
TU_3450	3400	Understory	Temp/RH	ABERG	13.11375	71.60747	2007–2009
Acjanaco	3487	Open	Manual WS	SENAMHI	13.19639	71.62000	2001–2007
TC_3600	3600	Understory	Temp/RH	ABERG	13.12313	71.61757	2007–2009
Qero	4131	Open	Automatic WS	Atrium	13.4533	71.1794	2006–2008

values measured. We then calculated the monthly and annual mean and standard deviation for each variable, for the period July 2007 through June 2008. We also report the absolute maximum and minimum temperature values recorded over the 2 yr+ measurement period. For manual weather stations, we averaged the recorded maximum and minimum temperatures for each day. Using data recorded every 10 min from our automatic weather stations, daily mean temperatures calculated as the mean of minimum and maximum daily temperatures were 0.5–1.0°C higher than those calculated as the mean of all temperature recordings (data not shown), suggesting that mean temperatures from the manual weather station data may be an overestimate compared to a mean from continuous data. From the manual micrometeorological station data we calculated annual mean temperatures with 95% confidence intervals from 2000–2008 to compare our 1 yr of data to the decadal trend. For each set of data, we calculated the daily temperature range as maximum – minimum temperature for each day and the mean daily range for each month. We also fit cubic smoothing splines (smooth.spline command in R version 2.12.2 ; R Development Core Team 2011) to mean hourly temperature data to visualize the diurnal patterns in temperature. Finally, for each month, we calculated mean daily and day and night lapse rates with respect to altitude for both the understory and above the canopy.

2.3.2. Humidity

Relative humidity was recorded at the automatic micrometeorological stations and understory sensors. Since relative humidity is temperature-dependent, vapor pressure (VP) and vapor pressure deficit (VPD) are better measures of the amount of atmospheric moisture and the moisture stress on plants, respectively (Anderson 1936). We therefore also calculated VP and VPD for each 10 min measurement period using Eqs. (5), (7), (12), and (14) of Yoder et al. (2005). We then calculated mean, daytime mean, nighttime mean, maximum, and minimum VPD on daily and monthly time scales. We also fit cubic smoothing splines to mean hourly VP and VPD values to visualize the diurnal patterns in humidity. Finally, we cal-

culated the percentage of measurement points where relative humidity was greater than 95%, and the percentage of measurement points where VPD was greater than 1 kPa by month, as metrics of fog occurrence and potential water stress for plants. Relative humidity values greater than 100% occurred in the understory sensors when they were saturated with liquid water. Because the relative humidity of the air likely dropped below 100% before the sensors dried out, we removed these points from the data (6.2% of understory data points) before any calculations were made. This procedure likely removed a greater proportion of high relative humidity values, such that the data presented here likely suggests a slightly drier environment than actually exists, but we think this preferable to setting these points to 100% relative humidity when some were likely lower.

2.3.3. Photosynthetically active radiation (PAR)

We calculated mean daily integrated PAR (400–700 nm; mol m^{-2} d^{-1}) for each month. To examine seasonal variation in diurnal trends, we fit cubic smoothing splines to measured PAR averaged over individual months. To calculate potential (clear sky) radiation, we fit cubic splines to the maximum PAR recorded during each month for each hour.

2.3.4. Rain

Rainfall totals were calculated on hourly, daily, monthly, and yearly timescales. Hourly mean rainfall was calculated for each month, the 4 wettest and driest months, and for a complete year for 4 automatic weather stations. Values were then fitted with a cubic smoothing spline to visualize diurnal patterns in rainfall. Patterns were similar at the different timescales, and only the wet and dry season averages are presented here. Total rainfall was calculated for each day, and for months with more than 25 d with data, total rain for each month was standardized to 30 d (monthly rain) = (total measured rain / number of days with data) × 30. For stations with rain totals for multiple years, we calculated 95% confidence intervals for mean annual precipitation.

2.3.5. Potential evapotranspiration (PET)

PET was calculated for 4 sites using the equations of Turc (1961) and Jensen & Haise (1963) as formulated by Fisher et al. (2009), who showed that both performed well in tropical forests, with the Turc equation slightly underestimating and the Jensen & Haise equation slightly overestimating evapotranspiration at 21 tropical forest sites with eddy-flux towers, although it is unclear whether they perform as well in montane cloud forests. Actual evapotranspiration (AET) can be underestimated in montane forests because of higher aerodynamic conductance in steep terrain (Holwerda et al. 2012) and because of greater interception losses in forests with greater canopy water storage due to large epiphyte mats and greater leaf area index (LAI; Muñoz-Villers et al. 2011). However, LAI generally decreases with altitude (Bruijnzeel et al. 2011), tending to lower AET at higher altitude. An analysis of AET is beyond the scope of this study.

2.3.6. Wind

We calculated daytime, nighttime, and overall mean wind speed on daily and monthly time scales. The poles on which the weather stations were mounted occasionally rotated, rendering the wind direction data unreliable over monthly scales, but we created individual day windrose plots to show general daily patterns in wind direction. We also present mean wind speed data for focal months and maximum wind gusts in relation to rainfall events.

2.3.7. Cold-air intrusions

To illustrate the propagation of cold-air intrusions in the study area, we present daily totals (rain and PAR), means (temperature and relative humidity), or maximum (wind gust) for the period April–July 2008.

3. RESULTS

We identified 3 seasonal periods, across which altitudinal patterns in microclimate changed. The wet season was the longest and most stable season running from November through March. April was transitional, and May through July formed the dry season, with a shallower lapse rate and increasing light and VPD with altitude. August was also transitional, followed by austral spring in September and October, characterized by a steeper lapse rate and declining light and VPD with altitude.

3.1. Temperature

Temperatures were higher and more variable during the day than at night, and above the canopy than in the understory (Table 2). Diurnal temperature range was similar across altitude for both above-canopy and the understory, although the temperature range was lower in the understory (Fig. 2b). A larger diurnal temperature range was recorded at stations in clearings than above the forest canopy, and the diurnal temperature range in the lowlands and above the tree line was lower than along the slope of the Andean front (Fig. 2b). Temperatures were higher in the wet season than the dry season, although the difference in mean temperature between the warmest (September) and coolest (June) months was generally less than 4°C, with greater variability at lower altitude (Fig. 2). During the dry season, temperatures were higher in the morning than in the afternoon, most strongly at higher altitude, while during the rest of the year, the temperature regime was more symmetric around a mid-day maximum (Fig. 3).

The overall lapse rate of the understory was similar to, but less variable than the above-canopy rate (Table S1; www.int-res.com/articles/suppl/c055p017_supp.pdf). Daytime lapse rates were shallower and more variable than nighttime lapse rates (Fig. 2). Predawn lapse rate, often measured in earlier work (Terborgh 1971, Bush et al. 2004), was similar to nighttime lapse rate (Table S1). The lapse rate varied throughout the year (Fig. 2), with the dry season having a shallow lapse rate, the austral spring having a much steeper lapse rate, and the wet season being intermediate and much less variable. Seasonal variation in lapse rate was associated with higher seasonal temperature variability at lower altitude (Fig. 2, Table 2).

3.2. Humidity

Relative humidity was high for much of the year, with values greater than 95% recorded during the majority of measurements during the wet season above the canopy (Fig. 4d). VP declined with altitude and had clear diurnal variation, but the diurnal pattern and differences between above-canopy and understory were fairly consistent throughout the year (Figs. 5 & 6). VPD was lower in the wet season, and the altitudinal trend switched direction from the dry season to the austral spring, with average VPD increasing with altitude in June but decreasing in September and January (Fig. 5). VPD was lower and more variable from site to site in the understory (Fig. 5), the variability likely associated with micro-

Table 2. Temperature in the Kosñipata Valley, showing mean ± SD of annual temperature (MAT), daytime (06:00–18:00 h), and nighttime (18:00–06:00 h) temperatures, as well as mean daily maximum and minimum temperatures (°C), and absolute maximum and minimum temperatures (°C) for July 2007 through June 2008, except for the sensors at 3000 m (June 2006 – May 2007) and 4130 m (January–December 2007). Absolute maximum and minimum temperatures are from the entire period that each sensor was installed

Altitude (m)	Location	No. days	MAT	Day MAT	Night MAT	Mean MaxT	Mean MinT	MaxT	MinT
1500	Canopy	347	18.09 ± 1.82	19.00 ± 2.10	17.17 ± 1.66	21.94 ± 2.46	15.80 ± 1.78	28.62	7.47
1500	Understory	329	17.41 ± 1.54	18.06 ± 1.72	16.77 ± 1.42	19.71 ± 1.99	15.58 ± 1.56	25.21	8.92
1750	Understory	360	15.84 ± 1.26	16.25 ± 1.36	15.43 ± 1.20	17.37 ± 1.55	14.47 ± 1.32	23.57	9.24
1840	Canopy	361	16.51 ± 1.59	17.23 ± 1.88	15.79 ± 1.43	20.03 ± 2.29	14.38 ± 1.61	25.50	6.71
1840	Understory	366	16.04 ± 1.32	16.69 ± 1.52	15.38 ± 1.20	18.73 ± 2.04	14.41 ± 1.33	24.17	8.52
2020	Understory	366	14.87 ± 1.13	15.41 ± 1.25	14.33 ± 1.09	17.22 ± 1.74	13.32 ± 1.20	22.37	8.63
2250	Understory	365	14.31 ± 1.19	15.62 ± 1.56	12.99 ± 1.02	18.34 ± 2.22	11.76 ± 1.16	25.33	7.82
2520	Understory	366	12.11 ± 0.97	12.61 ± 1.03	11.62 ± 0.99	13.88 ± 1.35	10.65 ± 1.11	26.34	6.97
2720	Canopy	365	11.80 ± 1.21	12.74 ± 1.50	10.85 ± 1.10	16.25 ± 2.22	9.53 ± 1.23	22.08	4.43
2720	Understory	343	11.10 ± 0.98	11.59 ± 1.01	10.61 ± 1.01	12.69 ± 1.19	9.69 ± 1.09	16.76	6.23
3000	Open	354	11.09 ± 1.21	12.72 ± 1.61	9.45 ± 1.13	15.88 ± 2.24	8.18 ± 1.27	21.74	3.59
3020	Understory	342	9.49 ± 1.02	10.26 ± 1.16	8.71 ± 1.03	11.72 ± 1.58	7.69 ± 1.13	16.37	2.56
3200	Understory	341	8.90 ± 1.02	9.69 ± 1.20	8.11 ± 0.97	11.62 ± 2.11	7.17 ± 1.04	18.63	3.56
3400	Canopy	313	8.42 ± 0.98	9.25 ± 1.23	7.58 ± 0.89	11.84 ± 1.76	6.25 ± 1.01	17.99	2.37
3400	Understory	341	7.66 ± 1.12	8.70 ± 1.26	6.62 ± 1.21	10.72 ± 2.54	5.55 ± 1.36	24.61	1.13
3600	Understory	289	6.46 ± 0.86	7.28 ± 0.79	5.65 ± 1.07	8.64 ± 0.96	4.46 ± 1.25	16.25	−1.13
4130	Open	331	4.79 ± 1.20	5.77 ± 1.22	3.81 ± 1.44	7.98 ± 1.46	2.14 ± 1.72	11.60	−5.40

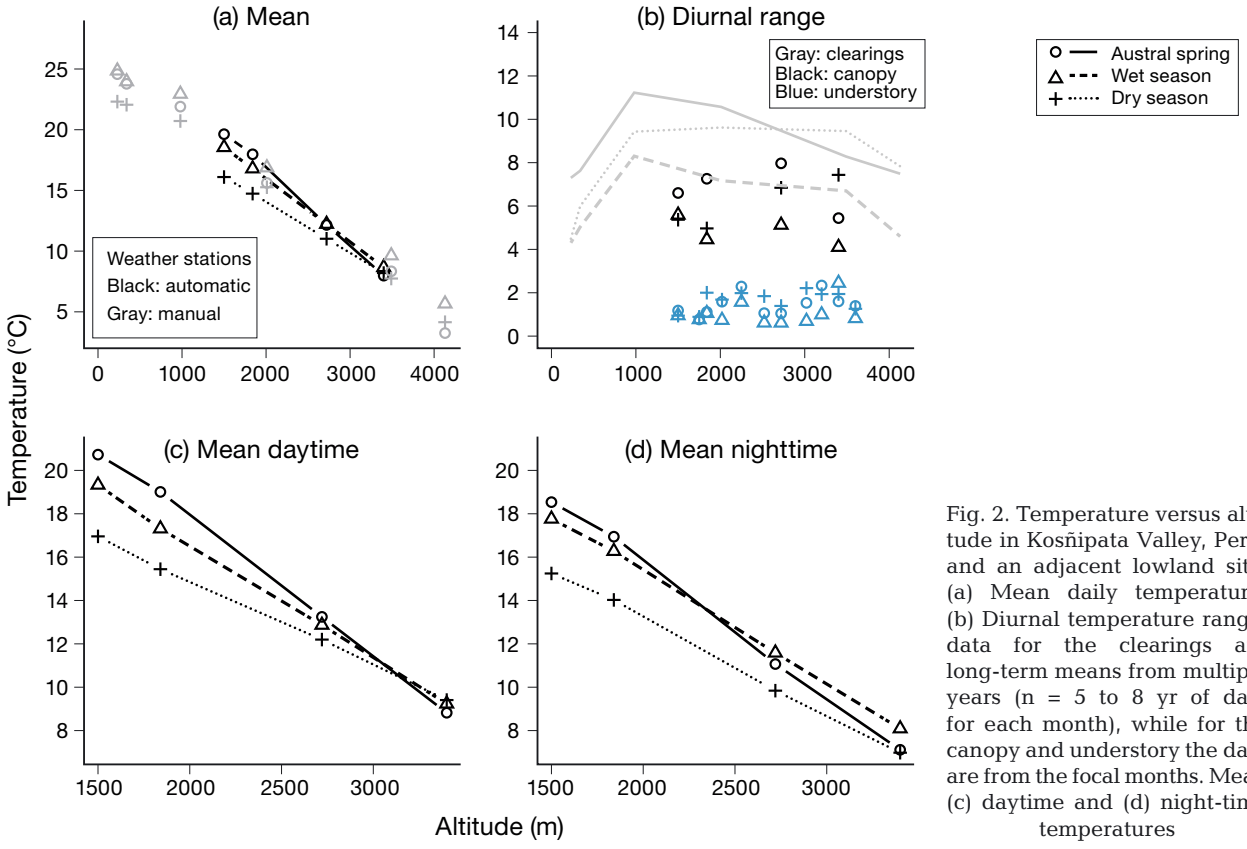

Fig. 2. Temperature versus altitude in Kosñipata Valley, Peru, and an adjacent lowland site. (a) Mean daily temperature. (b) Diurnal temperature range; data for the clearings are long-term means from multiple years (n = 5 to 8 yr of data for each month), while for the canopy and understory the data are from the focal months. Mean (c) daytime and (d) night-time temperatures

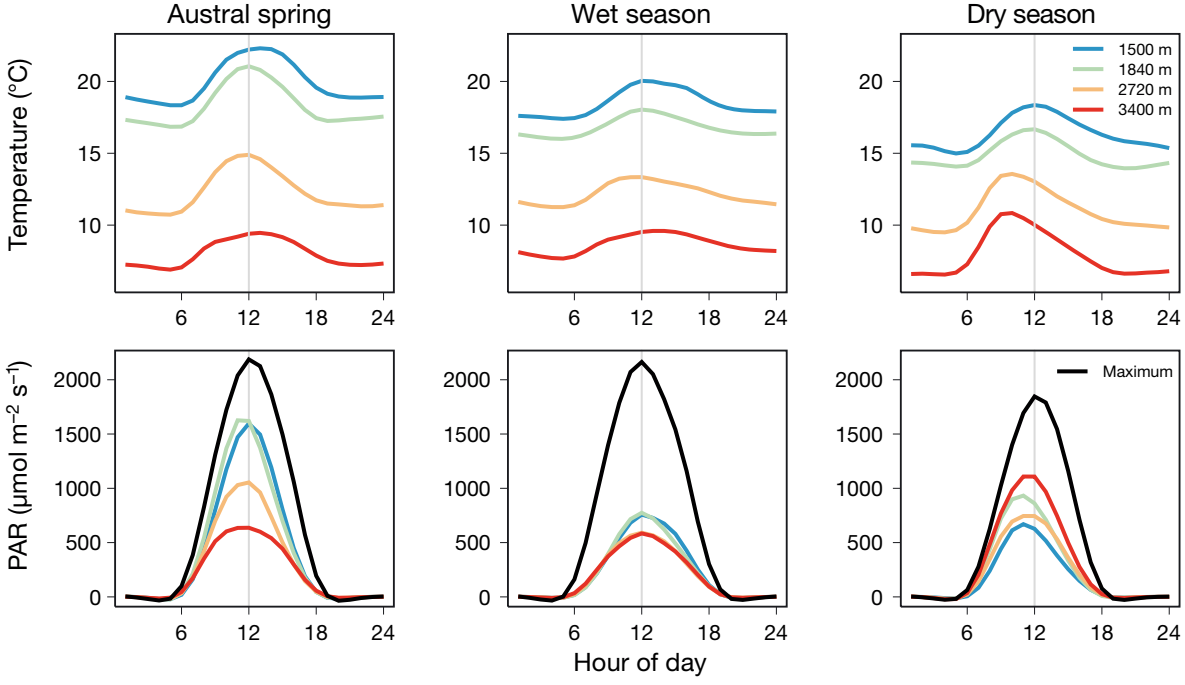

Fig. 3. Diurnal trends in temperature and instantaneous photosynthetically active radiation (PAR) during the austral spring (September) 2007, wet season (January) 2008, and dry season (June) 2008. Lines show a cubic spline fit to data for above-canopy weather stations at 4 elevations and the maximum values recorded for each hour

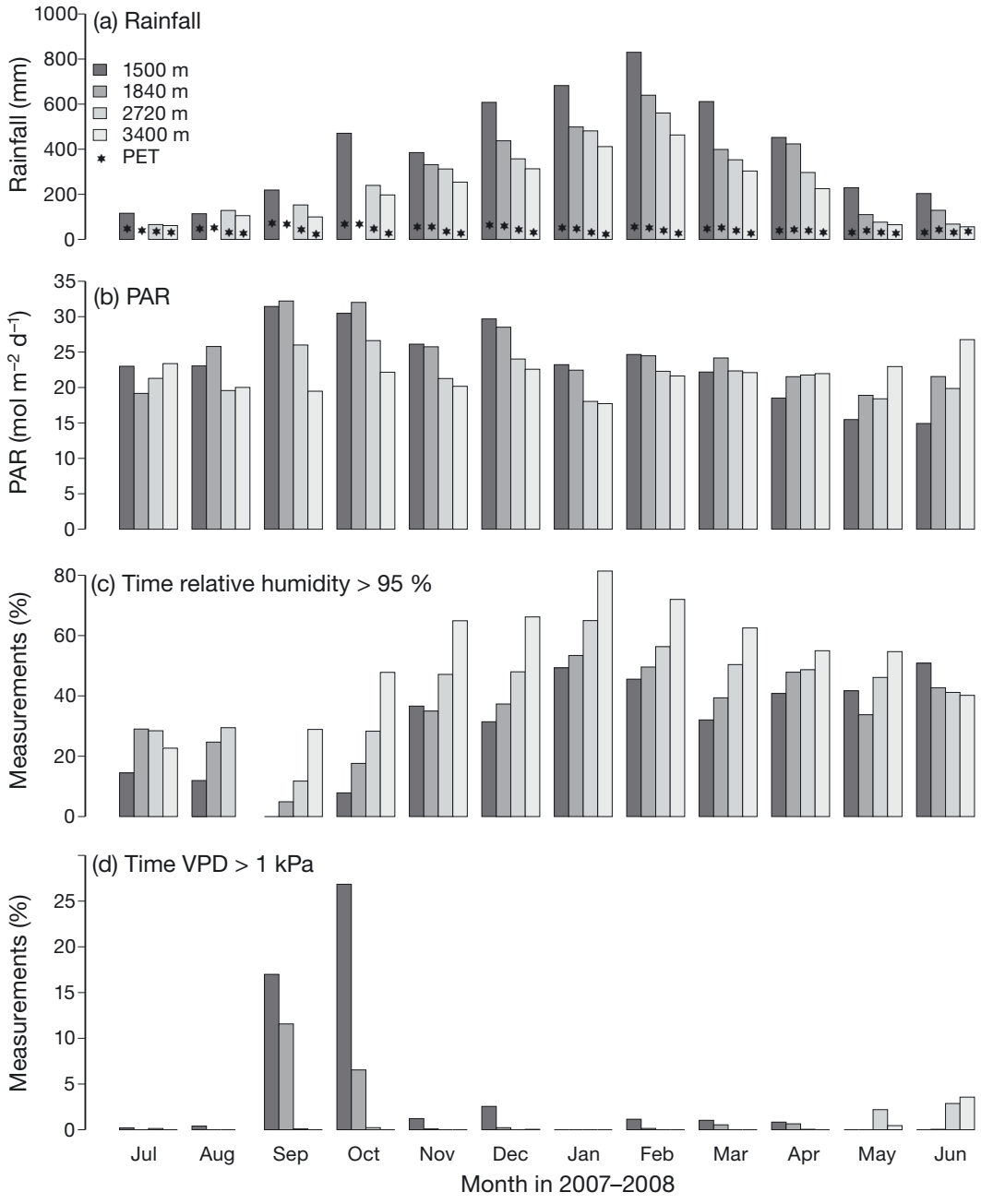

Fig. 4. (a) Rainfall standardized to 30 d mo^{-1} and potential evapotranspiration (PET) calculated using the Turc (1961) equation, (b) daily integrated photosynthetically active radiation (PAR), (c) percentage of measurements for which relative humidity was greater than 95%, and (d) the percentage of measurements for which vapor pressure deficit (VPD) was greater than 1 kPa in the Kosñipata Valley. Bars show data for above-canopy weather stations during a 1 yr period from July 2007 to June 2008

site placement of sensors. Diurnal patterns in VPD were strongest during the austral spring, weakest during the wet season, and stronger above the canopy than in the understory (Fig. 6). Periods when VPD was greater than 1 kPa (potentially stressful for plants) were also most common during the austral spring at lower altitudes (Fig. 4e).

3.3. Photosynthetically active radiation

For most of the year, PAR decreased with altitude (Fig. 4b). This pattern was reversed in the dry season (April–July), when cloudiness was lower at high altitudes. During the austral spring (September–October), when the highest light levels were attained

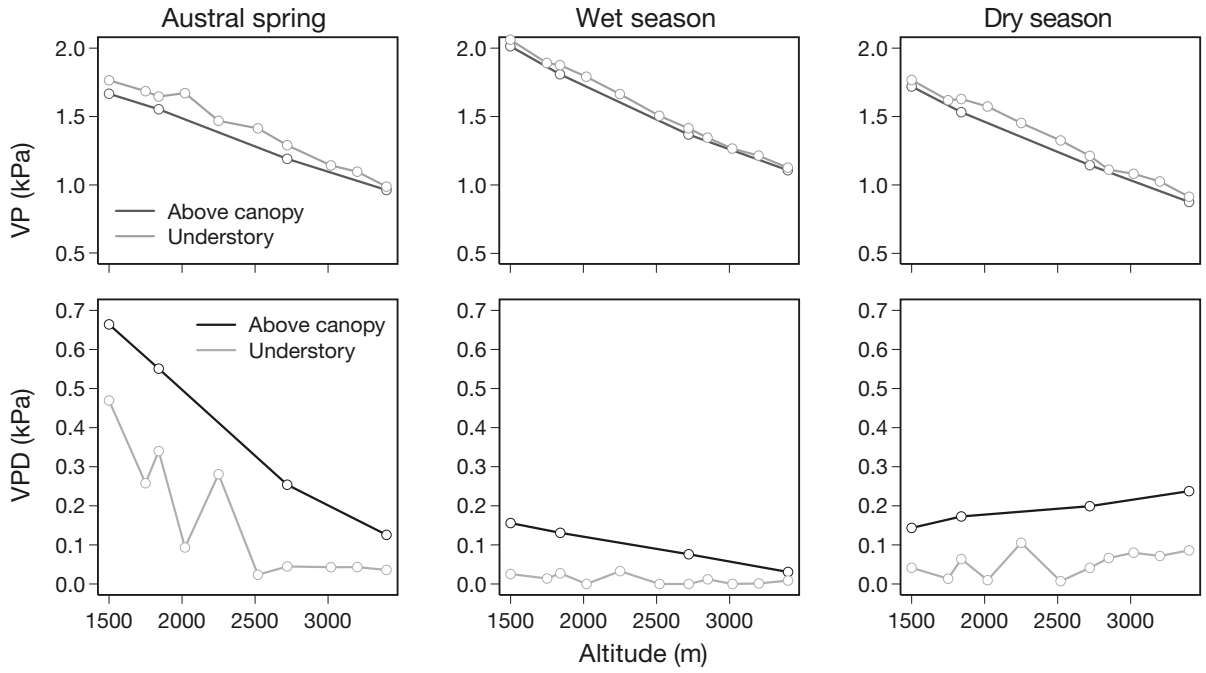

Fig. 5. Mean vapor pressure (VP) and vapor pressure deficit (VPD) plotted against altitude for 3 months in 2007–2008 in the Kosñipata Valley

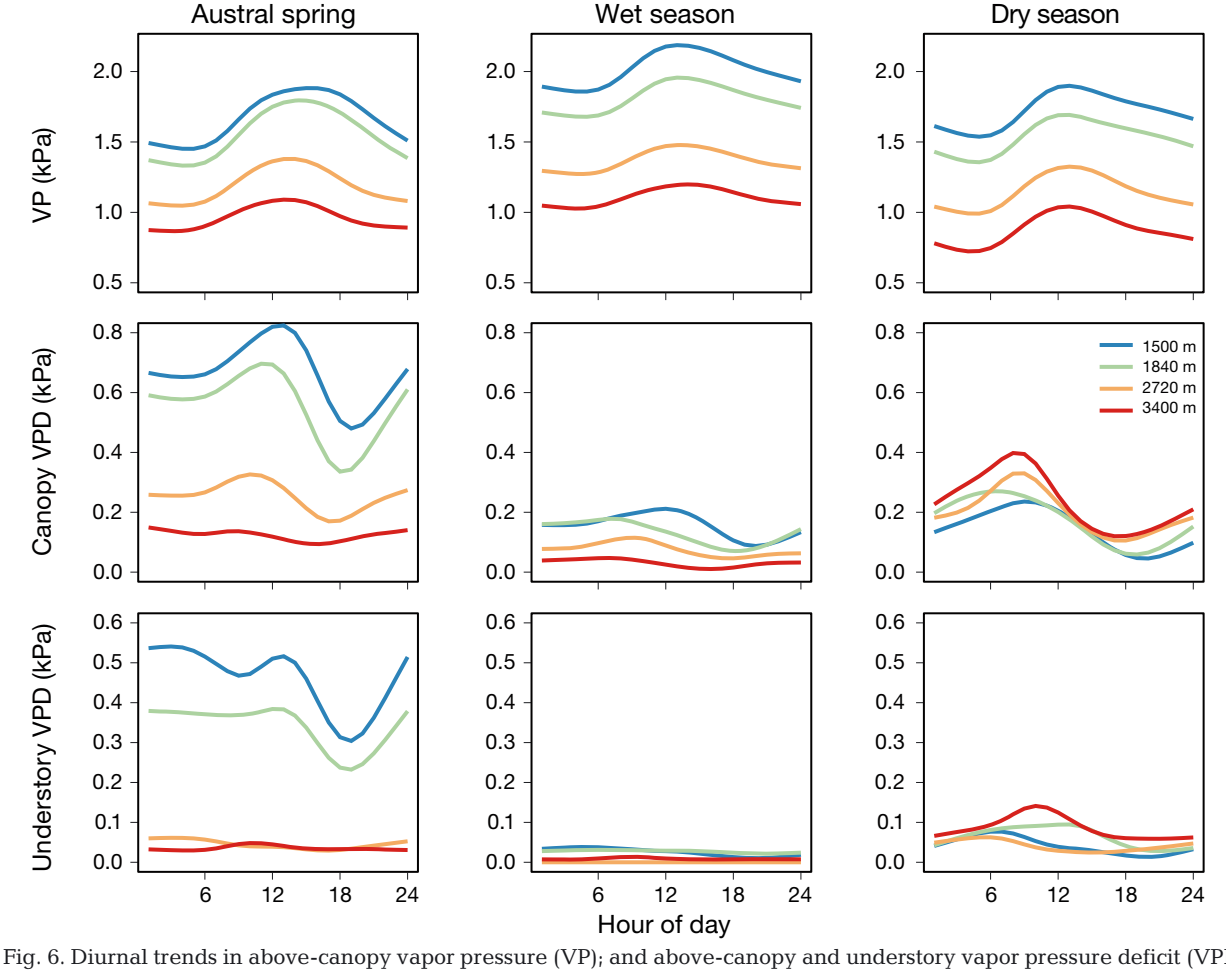

Fig. 6. Diurnal trends in above-canopy vapor pressure (VP); and above-canopy and understory vapor pressure deficit (VPD) for 3 months during the austral spring (September) 2007, wet season (January) 2008, and dry season (June) 2008. Lines show a cubic spline fit to data for 4 elevations

for all but the highest altitude, the gradient of decreasing PAR with altitude was strongest. Light levels remained high into the early wet season (November and December), before decreasing (Fig. 4b). Realized solar radiation was less than half of the maximum potential (clear sky) radiation at most altitudes, most of the year, and greater in the morning than in the afternoon, most strongly during the dry season (Fig. 3).

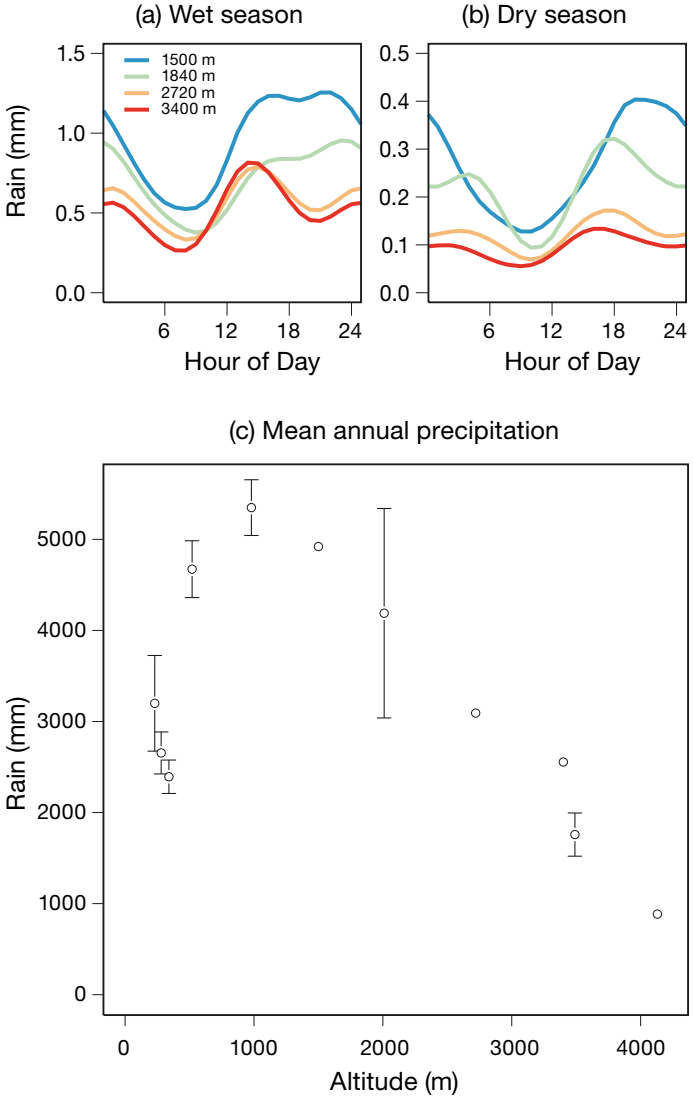

Fig. 7. Diurnal pattern of rainfall during the (a) wet (December to March) and (b) dry (May to August) seasons in the Kosñipata Valley. Lines show cubic splines fit to mean hourly rainfall values. (c) Mean annual precipitation across the altitudinal gradient in the Kosñipata Valley and nearby lowland and highland areas. Points with error bars ± 95% confidence intervals are stations with multiple years of data. See Table 1 and Fig. 1 for weather station locations and years of data collection

3.4. Rain

Highest rainfall was generally in January and February, with lowest totals in June and July (Fig. 4a). Diurnal patterns in rainfall were consistent across the year, with peak rainfall in the early afternoon, and a second peak overnight (Fig. 7a,b). These 2 peaks were most distinct at higher altitude, but merged to form 1 broad peak at lower altitude (Fig. 7a,b). Above 1000 m, rainfall declined monotonically with altitude at all times of the year, with precipitation ranging from >5000 mm yr^{-1} at 890 m to <1000 mm yr^{-1} at 4130 m (Fig. 7c). Inter-annual variability was greatest at 2010 m (Fig. 7c). Rainfall at 3400 m during 2007–2008 was higher than the mean annual rainfall from 2001–2006 at a station at 3490 m, either because rainfall was higher in 2007–2008, or because the station at 3490 m is in a more sheltered part of the Kosñipata Valley than the one at 3400 m. PET was similar when calculated using methods of both Turc (1961) and Jensen & Haise (1963) (less than 10 mm difference) in all months, and was always less than monthly rainfall at all altitudes (Fig. 4a; only values from the Turc equation are shown for clarity).

3.5. Wind

There was very little seasonal variation in wind direction, with patterns largely determined by local terrain and the upslope and downslope diurnal movement of air. Nighttime downslope winds were from the west and generally stronger than daytime northerly or easterly (depending on local terrain) upslope winds (Fig. 8). Mean wind speeds were higher at lower altitude, particularly during the austral spring (Fig. 9a). Strong wind gusts were rare, and most common at lower altitude, while high rainfall was more associated with strong winds at higher altitude (Fig. 9b).

3.6. Cold air incursions

The effects of cold air incursions from April–July 2008 in the Kosñipata Valley and adjacent lowlands depended on altitude (Fig. 10). Rain events at 1500 m were a consistent feature at the initiation of these events, although this rain did not always reach 3400 m and rain events in the lowlands were not always associated with these fronts. Cooling was greater at lower altitudes, leading to declining lapse rates during these periods. Ground-level cloud, indicated

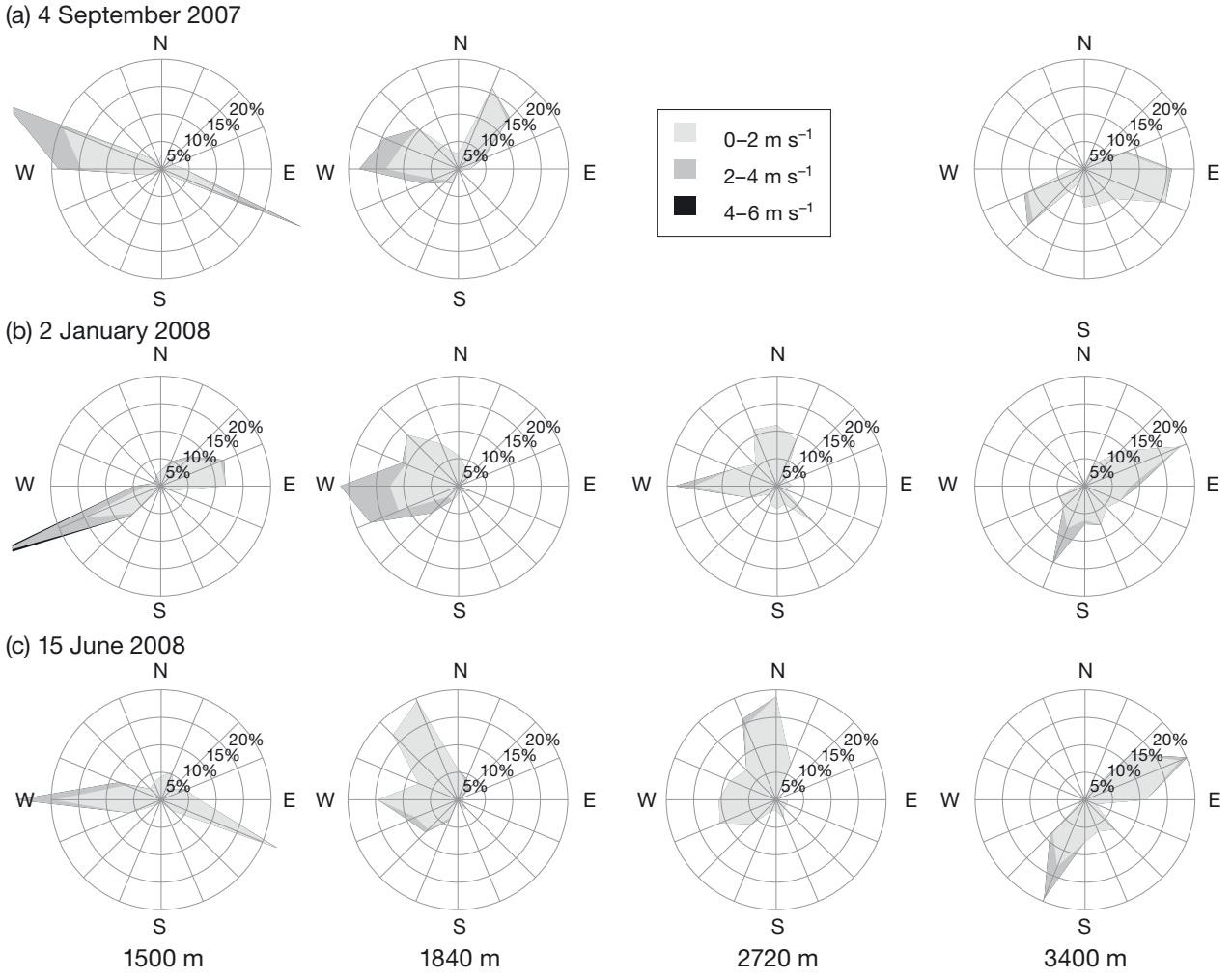

Fig. 8. Daily patterns of wind speed and direction for 3 dates (rows) at 4 different altitudes (columns). The radial axis represents percent of time the wind is blowing from a particular direction. No data were available for 2720 m on 4 September 2007. Westerly and southerly winds are nighttime downslope winds, while easterly and northerly winds are daytime upslope winds

by high relative humidity, was present at 1500 m but not at >2720 m where low relative humidity and high PAR indicated fewer clouds as the events developed. Wind gusts were of lower velocity during these events, particularly at 1500 m.

4. DISCUSSION

Diurnal and seasonal patterns and altitudinal trends in microclimate across the eastern Andean slope are determined by the combination of seasonal variation in moisture flux and solar radiation, interactions between moist air over the Amazon and dry air over the Andes, the adiabatic lapse rate, and the daily path of the sun.

4.1. Diurnal patterns

Diurnal patterns in microclimate in the Kosñipata Valley can be explained as the interaction of 2 air masses that meet along the east Andean front, and the diurnal variation in solar heating caused by the path of the sun. During the day, solar heating over the Amazon causes moist air to expand and push upslope, causing daytime upslope winds (Fig. 8) and higher VP (Fig. 6). Temperatures rise (Table 2; Fig. 3) along the Andean slope from direct heating and the influx of this warm, moist air. Rising moist air condenses into clouds, lowering light levels in the afternoon (Fig. 3) and causing a rain fall maximum (Fig. 7). After sunset, the flow of air reverses with cold, dry downslope winds (Fig. 8), and VP is lower

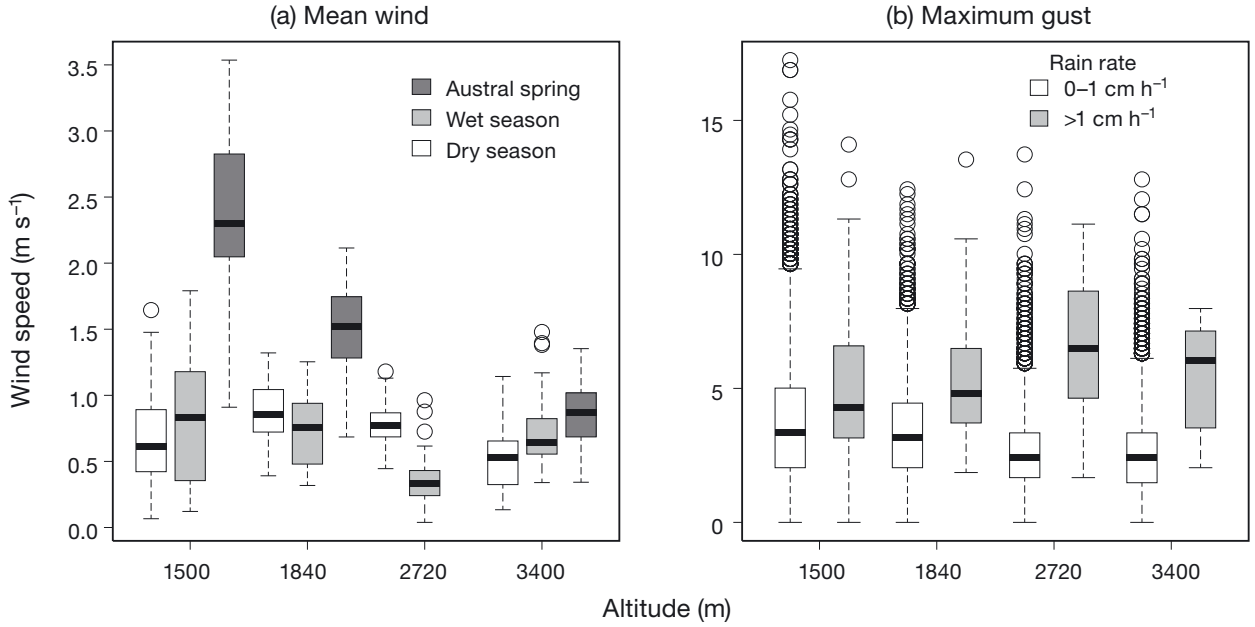

Fig. 9. (a) Monthly wind speed versus altitude in the Kosñipata Valley for 3 months, during the austral spring (September) 2007, wet season (January) 2008, and dry season (June) 2008; and (b) maximum wind gust versus altitude for time periods with or without heavy rainfall. Thick horizontal line shows the mean, boxes show quartiles, whiskers indicate extreme data points located not more than 1.5 times the interquartile range from the box, and circles show outliers

across the slope (Fig. 6). This sinking air displaces near-surface moist air at lower elevations, causing convection (Bendix et al. 2009), producing a second rainfall peak overnight, most strongly during the wet season (Fig. 7). At lower elevations, the afternoon peak is later and the night peak earlier, forming 1 broad peak (Fig. 7). Rainfall maxima in the afternoon and overnight have been observed at other Andean sites, with diurnal variability in the strength of low-level jets (Vernekar et al. 2003) and local topography being implicated in driving local patterns (Poveda et al. 2005). A plausible scenario for this pattern in the Kosñipata Valley is the afternoon peak being driven by the upslope flow of warm, moist air condensing as it cools, causing precipitation over higher elevations. As the air ascends above the height of land, the prevailing westerlies (Halladay 2012) force the rain clouds to the east, causing rainfall over lower altitudes. In contrast, nocturnal katabatic flow causes convection at the base of the slope, as shown for a site in Ecuador (Bendix et al. 2009), which then drifts west causing precipitation to propagate upslope.

4.2. Seasonality

Seasonality in microclimate along the east Andean slope appears to be largely related to 2 factors: seasonality in regional moisture flux caused by the strength of the SALLJ, and seasonality in solar radiation due to changes in solar angle. At ~13° S latitude, day length varies by less than 1.5 h throughout the year, while solar angle varies between 54.5° at the austral winter solstice and 90° in late October and mid-February. Thus, there is more available solar energy during the wet season than the dry season. However, the SALLJ strengthens during the austral summer (Marengo et al. 2004), and the increased moisture availability results in increased rainfall and cloudiness, limiting the amount of solar radiation reaching the ground (Fig. 4). PAR above the canopy peaks in September to December (Fig. 4), and temperature also peaks at this time, remaining high throughout the wet season (Fig. 2). Both of these patterns were also observed in Bolivia (Gerold et al. 2008). High temperatures and light levels result in high VPD, since atmospheric VP is fairly consistent throughout the year (Fig. 6). Higher energy availability during October through March facilitates the creation of stronger storms (Fig. 9).

4.3. Altitudinal trends

In contrast to oceanic islands such as Hawaii (Kitayama & Mueller-Dombois 1994, Leuschner 2000), most microclimate variables in this study show smooth trends with altitude. Instead of a step

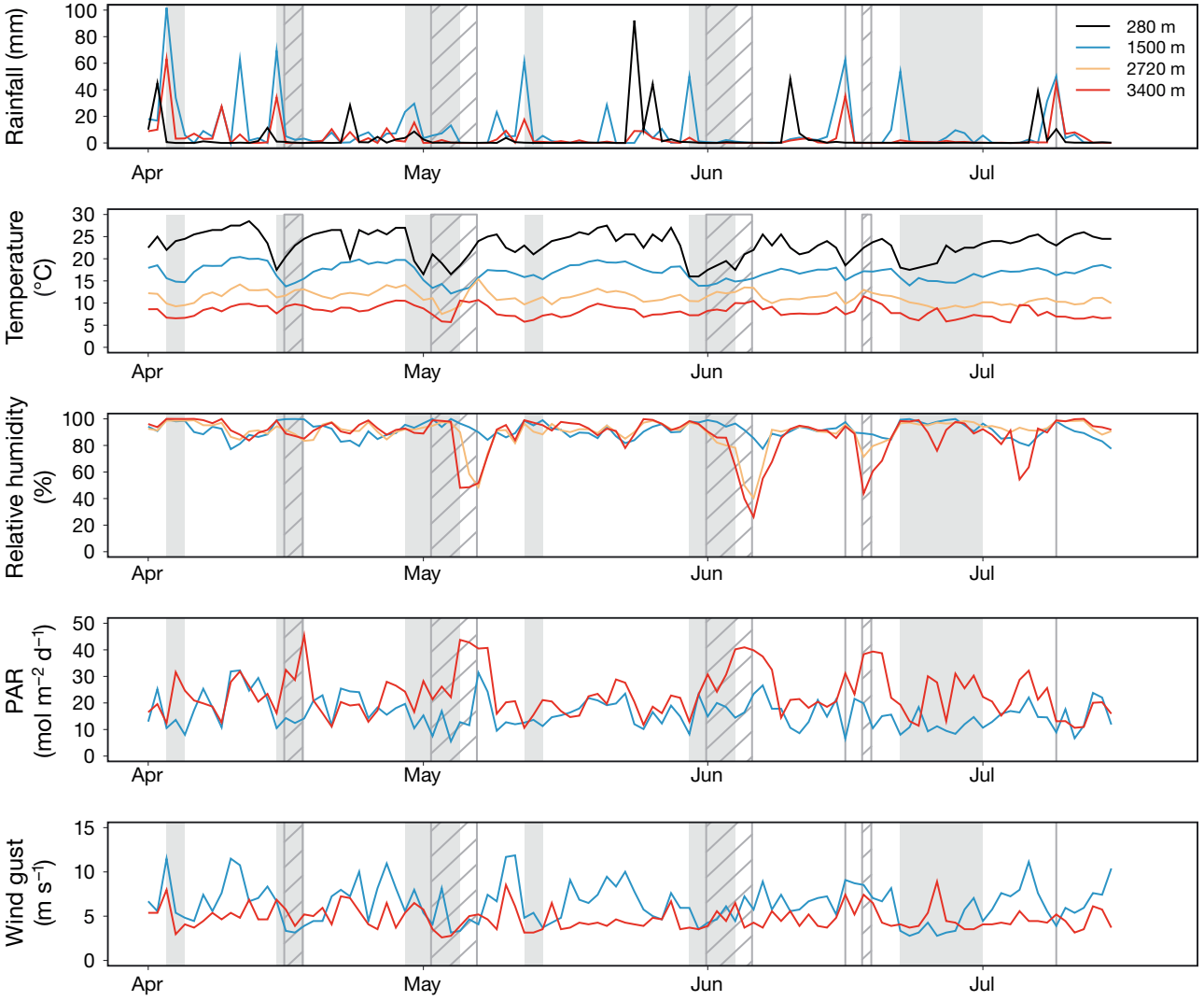

Fig. 10. Microclimate (daily mean values) from above-canopy weather stations in the Kosñipata Valley and a weather station at the Los Amigos Biological Station (280 m) for April–July 2008, showing anomalies due to cold air incursions. Gray areas indicate time periods when relative humidity was greater than 95 % at 1500 m, while the hatched areas indicate time periods when lapse rate was less than 3.3°C km^{-1} ±2 SD less than the mean lapse rate. PAR: photosynthetically active radiation

change in precipitation as in Hawaii (Kitayama & Mueller-Dombois 1994), annual precipitation decreases linearly with altitude above 1000 m (Fig. 7c). This is consistent with results from another Andean site in Colombia (Veneklaas & Van Ek 1990), while precipitation declined with altitude in Bolivia (Gerold et al. 2008) and was lower at 1890 m than at 2380 and 3060 m in Ecuador (Leuschner et al. 2007). VP (Fig. 5) and temperature (Fig. 2) also decline with altitude in our study area, as do PAR and VPD for most of the year, but during the middle of the dry season, the patterns for PAR and VPD are reversed (Figs. 4c & 5). In Bolivia, PAR also declined with altitude, but there was no gradient reversal during the dry season (Gerold et al. 2008). During the dry season, low cloud is often present at lower altitudes within the cloud forest, while dry Andean air dominates the upper altitudes, allowing higher light levels (Fig. 3) and raising VPD (Fig. 6). In contrast to temperate mountains where wind speed generally increases with altitude (McVicar et al. 2010), wind speed changes little with altitude over much of the year, and is higher at low altitude during the austral spring (Fig. 9). Rainfall was greater than calculated PET for all altitudes during the year of observation, at monthly scales. Although AET may be underestimated at monthly scales in this humid system (see Materials and Methods), we did not measure occult precipitation, which would further increase the precipitation surplus. We conclude

that moisture stress is unlikely between 1500 and 3500 m under current climate conditions.

4.4. Cold-air incursions

Cold air incursions progressed from low to high altitude, with temperature declines attenuating along the gradient (Fig. 10). Cloud at low altitude may suppress the normal daytime upslope flow of warm, moist air, suggested by a trend toward lower maximum wind gusts during incursions, while declines in relative humidity and higher light levels at higher altitudes may have been the result of downslope incursions of dry Andean air made possible by the lack of counterbalancing upslope flow. Increased sunshine led to a slight increase in temperature at 3400 m during these events.

4.5. Putative cloud base

Relatively smooth changes in microclimate across the altitudinal gradient contrast with sharper changes in ecosystem structure, suggesting that thresholds in microclimatic variables may be important. We did not see a sharp change in either light levels (Fig. 4c) or humidity (Fig. 5) above 1500 m that would indicate a consistent cloud base, although during the austral spring, PAR, temperature, and VPD were higher at 1500 and 1840 m in the year for which we had continuous data (Figs. 3 & 6). A humidity threshold may contribute to the change in biomass and productivity above 1500 m. VPD below 0.2 kPa can promote growth of fungal pathogens (Grange & Hand 1987), and VPD is rarely above this level above 1500 m during the wet season (Fig. 6). Fungal pathogens and reduced transpiration (Motzer et al. 2005) may contribute to lower productivity above 1500 m for trees, while these same moist conditions are favorable for bryophyte growth. During the dry season, VPD values can exceed 1 kPa at 1500 m and less frequently at 1840 m. Photosynthesis in cloud forest trees begins to be limited by moisture stress at VPD values of 1 to 1.2 kPa (Cunningham 2004, Motzer et al. 2005), so dry season water stress may contribute to changes in forest properties between 1500 and 2000 m.

4.6. Tree line

In the Kosñipata Valley, the tree line is located at ~3500 m, although scattered patches of trees are present above this. During the dry season, the usual gradient in solar radiation and evaporative demand switches direction, with PAR and VPD increasing with altitude (Figs. 4c, 5 & 6). High solar radiation and higher VPD at high altitude, particularly during cold air incursions (see above), promote desiccation of the vegetation, supporting fire, which in extreme years can reach as low as 2400 m (M. R. Silman pers. obs.). Topographic positions that accumulated cold air were treeless in Ecuador (Bader & Ruijten 2008), and the occasional freezing temperatures above 3400 m (Table 2) in our study area may inhibit tree regeneration and influence the location of the tree line. A temperature inversion that can descend as low as 3000 m in the dry season (Halladay 2012) may also play a role, as it does in Hawaii (Crausbay & Hotchkiss 2010).

5. CONCLUSIONS

The micrometeorological dataset presented here, including measurements of temperature, rainfall, humidity, sunlight, and wind, gives a unique description of the climate along an altitudinal gradient in the eastern Andes, one of the world's most biologically diverse forest ecosystems. Cloud dynamics are strongly implicated as a driver of the diurnal and seasonal patterns, as well as the altitudinal trends described. Somewhat surprisingly, we found little evidence for a consistent cloud base and top, often assumed to control cloud forest structure and function, although the short time series of our data (<3 yr) does not preclude the existence of these features. Instead, smooth changes in micrometeorological variables across the altitudinal gradient suggest a cloud immersion zone where cloud frequency varies smoothly, and thresholds in cloud frequency, rather than presence or absence of clouds, may be more important in determining forest structure and function.

Acknowledgements. This paper is a product of ABERG (http://andesconservation.org). We thank the Servicio Nacional de Meteorolgía e Hidrología del Perú (www.senamhi.gob.pe) and the Botanical Research Institute of Texas (atrium.andesamazon.org) for climate station data. Special thanks go to N. Salinas Revilla at the Universidad Nacional de San Antonio Abad in Cusco, Peru. Support came from the Gordon and Betty Moore Foundation's Andes to Amazon initiative, NSF DEB-0237684, and NSF EAR-0711414. INRENA, SERNANP, and personnel of Manu National Park, Peru, provided assistance with logistics. We thank the Amazon Conservation Association and the Cock-of-the-Rock Lodge for providing logistical support. Comments by K. Halladay, J. Fisher, and 2 anonymous reviewers greatly improved the manuscript.

LITERATURE CITED

Aiba SI, Kitayama K (2002) Effects of the 1997-98 El Niño drought on rain forests of Mount Kinabalu, Borneo. J Trop Ecol 18:215–230

Anderson DB (1936) Relative humidity or vapor pressure deficit. Ecology 17:277–282

Bader MY, Ruijten JJA (2008) A topography-based model of forest cover at the alpine tree line in the tropical Andes. J Biogeogr 35:711–723

Bendix J, Trachte K, Cermak J, Rollenbeck R, Nauss T (2009) Formation of convective clouds at the foothills of the tropical eastern Andes (South Ecuador). J Appl Meteorol Climatol 48:1682–1695

Bruijnzeel LA, Mulligan M, Scatena FN (2011) Hydrometeorology of tropical montane cloud forests: emerging patterns. Hydrol Process 25:465–498

Bubb P, May I, Miles L, Sayer J (2004) Cloud forest agenda. UNEP-WCMC, Cambridge

Bush MB, Silman MR, Urrego DH (2004) 48,000 years of climate and forest change in a biodiversity hot spot. Science 303:827–829

Cowling SA, Shin Y, Pinto E, Jones CD (2008) Water recycling by Amazonian vegetation: coupled versus uncoupled vegetation-climate interactions. Philos Trans R Soc Lond B Biol Sci 363:1865–1871

Crausbay SD, Hotchkiss SC (2010) Strong relationships between vegetation and two perpendicular climate gradients high on a tropical mountain in Hawai'i. J Biogeogr 37:1160–1174

Cunningham SC (2004) Stomatal sensitivity to vapour pressure deficit of temperate and tropical evergreen rainforest trees of Australia. Trees (Berl) 18:399–407

Doan TM (2004) Extreme weather events and the vertical microhabitat of rain forest anurans. J Herpetol 38: 422–425

Fisher JB, Malhi Y, Bonal D, Da Rocha HR and others (2009) The land-atmosphere water flux in the tropics. Glob Change Biol 15:2694–2714

Fleischbein K, Wilcke W, Valarezo C, Zech W, Knoblich K (2006) Water budgets of three small catchments under montane forest in Ecuador: experimental and modelling approach. Hydrol Process 20:2491–2507

Foster P (2001) The potential negative impacts of climate change on tropical montane cloud forests. Earth Sci Rev 55:73–106

Garreaud RD (2000) Cold air incursions over subtropical South America: mean structure and dynamics. Mon Weather Rev 128:2544–2559

Garreaud RD, Vuille M, Compagnucci R, Marengo J (2009) Present-day South American climate. Palaeogeogr Palaeoclimatol Palaeoecol 281:180–195

Gentry AH (1988) Tree species richness of upper Amazonian forests. Proc Natl Acad Sci USA 85:156–159

Gerold G, Schawe M, Bach K (2008) Hydrometeorologic, pedologic and vegetation patterns along an elevational transect in the montane forest of the Bolivian Yungas. Erde 139:141–168

Giambelluca TW, Martin RE, Asner GP, Huang MY and others (2009) Evapotranspiration and energy balance of native wet montane cloud forest in Hawai'i. Agric For Meteorol 149:230–243

Girardin CAJ, Mahli Y, Aragao LEOC, Mamani M and others (2010) Net primary productivity allocation and cycling of carbon along a tropical forest elevational transect in the Peruvian Andes. Glob Change Biol 16: 3176–3192

Gomez-Peralta D, Oberbauer SF, McClain ME, Philippi TE (2008) Rainfall and cloud-water interception in tropical montane forests in the eastern Andes of Central Peru. For Ecol Manag 255:1315–1325

Grange RI, Hand DW (1987) A review of the effects of atmospheric humidity on the growth of horticultural crops. J Hortic Sci 62:125–134

Grubb PJ (1977) Control of forest growth and distribution on wet tropical mountains: with special reference to mineral nutrition. Annu Rev Ecol Syst 8:83–107

Grubb PJ, Whitmore TC (1966) A comparison of montane and lowland rain forest in Ecuador. II. The climate and its effects on the distribution and physiognomy of the forests. J Ecol 54:303–333

Halladay K (2012) Cloud characteristics of the Andes/Amazon transition zone. PhD thesis, University of Oxford

Herzog SK, Martínez R, Jørgensen PM, Tiessen H (eds) (2011) Climate change and biodiversity in the tropical Andes. Inter-American Institute for Global Change Research (IAI) and SCOPE, São José dos Campos, SP, Brazil

Holwerda F, Bruijnzeel LA, Munoz-Villers LE, Equihua M, Asbjornsen H (2010) Rainfall and cloud water interception in mature and secondary lower montane cloud forests of central Veracruz, Mexico. J Hydrol (Amst) 384: 84–96

Holwerda F, Bruijnzeel LA, Scatena FN, Vugts HF, Meesters A (2012) Wet canopy evaporation from a Puerto Rican lower montane rain forest: the importance of realistically estimated aerodynamic conductance. J Hydrol (Amst) 414-415:1–15

Jarvis A, Mulligan M (2011) The climate of cloud forests. Hydrol Process 25:327–343

Jensen ME, Haise JR (1963) Estimating evapotranspiration from solar radiation. J Irrig Drain Div 89:15–41

Killeen TJ, Douglas M, Consiglio T, Jorgensen PM, Mejia J (2007) Dry spots and wet spots in the Andean hotspot. J Biogeogr 34:1357–1373

Kitayama K, Mueller-Dombois D (1994) An altitudinal transect analysis of the windward vegetation on Haleakala, a Hawaiian island mountain. 1. Climate and soils. Phytocoenologia 24:111–133

Korner C (1998) A re-assessment of high elevation treeline positions and their explanation. Oecologia 115:445–459

Leigh EG Jr (1975) Structure and climate in tropical rain forest. Annu Rev Ecol Syst 6:67–86

Leuschner C (2000) Are high elevations in tropical mountains arid environments for plants? Ecology 81:1425–1436

Leuschner C, Moser G, Bertsch C, Roderstein M, Hertel D (2007) Large altitudinal increase in tree root/shoot ratio in tropical mountain forests of Ecuador. Basic Appl Ecol 8:219–230

Lomolino MV (2001) Elevation gradients of species-density: historical and prospective views. Glob Ecol Biogeogr 10: 3–13

Loope LL, Giambelluca TW (1998) Vulnerability of island tropical montane cloud forests to climate change, with special reference to East Maui, Hawaii. Clim Change 39: 503–517

Marengo JA, Soares WR, Saulo C, Nicolini M (2004) Climatology of the low-level jet east of the Andes as derived from the NCEP-NCAR reanalyses: characteristics and temporal variability. J Clim 17:2261–2280

Martinez R, Ruiz D, Andrade M, Blacutt L and others (2011) Synthesis of the climate of the tropical Andes. In: Herzog SK, Martinez R, Jørgensen PM, Tiessen H (eds) Climate change and biodiversity in the tropical Andes. Inter-American Institute for Global Change Research (IAI) and SCOPE, São José dos Campos, SP, Brazil, p 97–109

McVicar TR, Van Niel TG, Roderick ML, Li LT, Mo XG, Zimmermann NE, Schmatz DR (2010) Observational evidence from two mountainous regions that near-surface wind speeds are declining more rapidly at higher elevations than lower elevations: 1960-2006. Geophys Res Lett 37:L06402

Motzer T, Munz N, Kuppers M, Schmitt D, Anhuf D (2005) Stomatal conductance, transpiration and sap flow of tropical montane rain forest trees in the southern Ecuadorian Andes. Tree Physiol 25:1283–1293

Muñoz-Villers LE, Holwerda F, Gómez-Cárdenas M, Equihua M and others (2011) Water balances of old-growth and regenerating montane cloud forests in central Veracruz, Mexico. J Hydrol (Amst) 462-463:53–66

Myers N, Mittermeier RA, Mittermeier CG, da Fonseca GAB, Kent J (2000) Biodiversity hotspots for conservation priorities. Nature 403:853–858

Nadkarni NM, Solano R (2002) Potential effects of climate change on canopy communities in a tropical cloud forest: an experimental approach. Oecologia 131:580–586

Neelin JD, Munnich M, Su H, Meyerson JE, Holloway CE (2006) Tropical drying trends in global warming models and observations. Proc Natl Acad Sci USA 103:6110–6115

Patterson BD, Stotz DF, Solari S (2006) Mammals and birds of the Manu Biosphere Reserve, Peru. Fieldiana Zool 110:1–49

Pinto E, Shin Y, Cowling SA, Jones CD (2009) Past, present and future vegetation-cloud feedbacks in the Amazon Basin. Clim Dyn 32:741–751

Pounds JA, Fogden MPL, Campbell JH (1999) Biological response to climate change on a tropical mountain. Nature 398:611–615

Poveda G, Mesa OJ, Salazar LF, Arias PA and others (2005) The diurnal cycle of precipitation in the tropical Andes of Colombia. Mon Weather Rev 133:228–240

R Development Core Team (2011) R: a language and environment for statistical computing. R Foundation for Statistical Computing, Vienna

Sarmiento FO, Frolich LM (2002) Andean cloud forest tree lines — naturalness, agriculture and the human dimension. Mt Res Dev 22:278–287

Smith WK, Germino MJ, Johnson DM, Reinhardt K (2009) The altitude of alpine treeline: a bellwether of climate change effects. Bot Rev 75:163–190

Still CJ, Foster PN, Schneider SH (1999) Simulating the effects of climate change on tropical montane cloud forests. Nature 398:608–610

Terborgh J (1971) Distribution on environmental gradients: theory and a preliminary interpretation of distributional patterns in avifauna of Cordillera Vilcabamba, Peru. Ecology 52:23–40

Turc L (1961) Estimation of irrigation water requirements, potential evapotranspiration: a simple climatic formula evolved up to date. Ann Agron 12:13–49

Veneklaas EJ, Van Ek R (1990) Rainfall interception in two tropical montane rain forests, Colombia. Hydrol Process 4:311–326

Vernekar AD, Kirtman BP, Fennessy MJ (2003) Low-level jets and their effects on the South American summer climate as simulated by the NCEP Eta Model. J Clim 16: 297–311

Vitousek PM (1998) The structure and functioning of montane tropical forests: control by climate, soils, and disturbance. Ecology 79:1–2

Vuille M, Francou B, Wagnon P, Juen I, Kaser G, Mark BG, Bradley RS (2008) Climate change and tropical Andean glaciers: past, present and future. Earth Sci Rev 89:79–96

Yoder RE, Odhiambo LO, Wright WC (2005) Effects of vapor-pressure deficit and net-irradiance calculation methods on accuracy of standardized Penman-Monteith equation in a humid climate. J Irrig Drain Eng 131: 228–237

Editorial responsibility: Tim Sparks, Cambridge, UK

Submitted: November 15, 2011; Accepted: July 25, 2012
Proofs received from author(s): October 31, 2012